MEASUREMENTS ON AN ENCLOSED VORTEX IN AN AXIAL MAGNETIC FIELD

V. G. Zhilin, A. N. Zagidullin, and V. B. Levin

UDC 537.84

Detailed theoretical and experimental studies have been made on rotating flows of homogeneous conducting liquids at small Reynolds numbers with the flow bounded by insulating planes perpendicular to a uniform external magnetic field, or by cylindrical side walls; less is known about enclosed rotating flows in which the lateral boundaries are far from the walls. The magnetohydrodynamic phenomena governing the structure and stability have been considered [1], where it was shown that free shear layers develop from the lines of discontinuity in the boundary conditions along the magnetic lines of force, the width being

$$\delta_{\parallel}(z) \sim z\,\mathrm{Ha}_z^{-1/2} = [(\sigma/\mu)^{1/2}B]^{-1/2}z^{-1/2}.$$

Here z is the coordinate in the field direction, σ and μ are conductivity and viscosity, B induction, and $\mathrm{Ha}_z = (\sigma/\mu)^{1/2}Bz$ the Hartmann number, defined with respect to z. If the rotation is due to an axial magnetic field interacting with a radial current from an external source, the current is closed [1] along the longitudinal and Hartmann layers (Fig. 1). Outside these layers, the flow is potential, $v \sim 1/r$, and the applied electric field is balanced by the induced one, $\partial\varphi/\partial r = vB$, where φ is the electric-field potential, v azimuthal velocity, and r radial coordinate. If h is the flow scale in the field direction, then for $\mathrm{Ha}_h \gg 1$ we have $\delta_{\parallel}/\delta_{\perp} \sim \mathrm{Ha}_h^{1/2} \gg 1$, where $\delta_{\perp} \sim h\mathrm{Ha}_h^{-1}$ is the Hartmann layer thickness. Consequently [1], the resistivity and dissipation in the longitudinal layers for $\mathrm{Ha}_h \gg 1$ are negligible by comparison with those in the Hartmann layer (the ratio is $\sim(\mathrm{Ha}^*)^{-1/2}$, where the modified Hartmann number is $\mathrm{Ha}^* = \mathrm{Ha}_h b^2/2h^2 = (\sigma/\mu)^{1/2}Bb^2/2h$, where b is the rotating layer width [2, 3]). Here $\mathrm{Ha}^* = (\sigma/\mu)^{1/2}BR^2/2h$.

1. Figure 1 shows the apparatus. The cylindrical stainless-steel vessel 1 is filled with indium–gallium–tin alloy and has internal diameter 169 mm and is coaxial in the solenoid 2. The magnetic field is uniform within 5% within the working part 400 mm long. The current is supplied by a TES-14 dc source to the metal via the copper wire 3 and ring electrode 4. The wire is insulated with polyvinyl chloride and has a diameter of 2.8 mm. A length of ~3 mm on wire 5 is bared, and this and the ring electrode lie in the mid-plane of the solenoid. The ring electrode is insulated from the liquid metal, apart from a cylindrical belt 6 having radius R = 30.5 mm and height 2 mm. The insulated tube 7 bears the lucite disk 8 immersed to a given depth, which contains 16 probes 9 for measuring the potential, which are made of 0.1 mm copper wire with lacquer insulation. The ends of the wires in contact with the liquid metal are 4 mm from the disk (outside the Hartmann layer). Lead 3 passes through a hole 3 mm in diameter in plate 8 and tube 7. The leads soldered to the probes are brought out through the cavity in disk 8 and tube 7.

The radial potential distributions have been measured at various distances z from the plane of the electrodes by means of the rotating probe fitted into tube 10 and the arm 11, through which the insulated lead passes. The radial coordinate for the end in contact with the liquid was determined from the angle of rotation in tube 10. Lead 3 passes through a hole in the lower lucite disk 12 into tube 13 and is tensioned by the rubber band 14. Tubes 7 and 13 insulated from the metal prevent the current flowing through the gap between lead 3 and the edges of the holes in plates 8 and 12. The lower part of Fig. 1 shows the current circuit via the longitudinal layers 15 and Hartmann layer 16 (thickness exaggerated in the figure), as well as the general azimuthal velocity pattern v(r).

2. Measurements were made with B = 0.02-0.4 T, distance between disks h = 48-280 mm, and electrode currents I = 35-300 mA, where we recorded $\varphi(r)$ at various distances z from the electrode plane (in the stationary state) as well as the time course of φ for one of the probes 9 near the axis of the working part outside the longitudinal layer (in the tran-

Translated from Magnitnaya Gidrodinamika, No. 3, pp. 135-138, July-September, 1988. Original article submitted December 11, 1987; revision submitted January 25, 1988.

 0024-998X/88/2403-0382$12.50

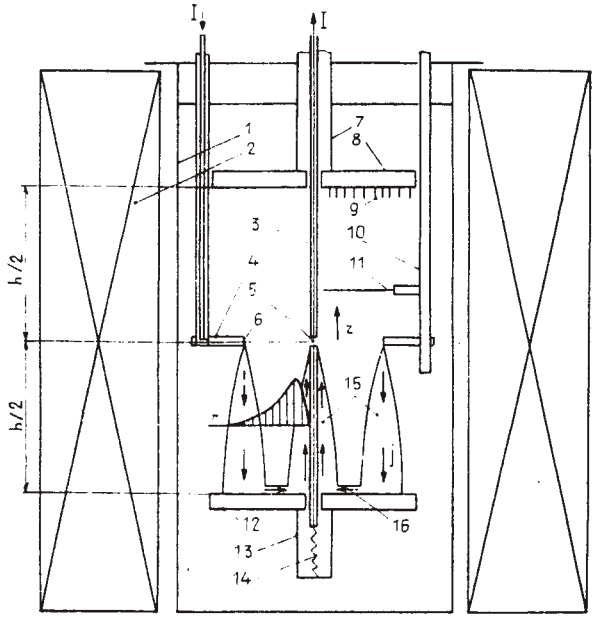

Fig. 1

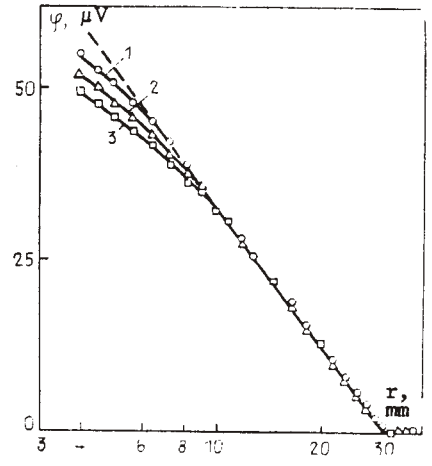

Fig. 2

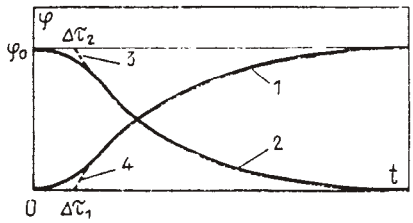

Fig. 3

Fig. 1. Apparatus, explanation in text.

Fig. 2. Potential φ as a function of radius r for B = 0.24 T, h = 140 mm, Ha* = 23, and z = 16 (1), 32 (2), 44 mm (3); dashed line – extrapolation corresponding to $v \sim 1/r$.

Fig. 3. Potential change proportional to velocity change on vortex acceleration and decay: 1) acceleration; 2) decay; 3) extrapolated exponential part of curve 2; 4) extrapolated exponential part of curve 1.

sient states after current switching). In both cases, the potential is reckoned relative to that of a probe placed outside the region of liquid motion. The measurements in the stationary state were made with an Shch-300 voltmeter, while in the transient states, the signals were recorded with an F 116/1 microvoltmeter and N 3031/4 pen recorder. The sensitivities of these instruments were almost constant in the range 0-0.5 Hz. The current was chosen to give the subcritical state close to the stability boundary. The maximum speed of v_m was 0.5-4 cm/sec.

Figure 2 shows φ as a function of r for various z. Similar curves were recorded for other B and h, and in accordance with the theory [1], they indicate that there is a poten-

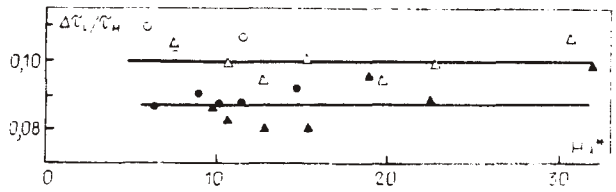

Fig. 4. Structuring time as a function of Ha* for h/2R = 2.3 (Δ, ▲) and 4.6 (○, ●) on acceleration (Δ and ○) and on decay (▲ and ●); solid line – corresponding averaged values.

Fig. 5. Acceleration time-constant τ_i (i = 1) and decay constant (i = 2) as functions of Ha*: 1) acceleration for h/2R = 1.6; 2, 3) decay for h/2R = 1.6, and 0.8 correspondingly; 4) [3, 5] data.

tial core having the velocity distribution $v \sim 1/r$ between the longitudinal layers, whose width decreases as z increases but which increases with B (this is due to the width of the longitudinal layers being dependent on z and B). A stationary state close to that here has been considered theoretically in [4].

One uses the flow homogeneity in z for Ha* $\gg$ 1 and the dissipation expression for unit area of the Hartmann layer, $D = (\sigma\mu)^{1/2}Bv^2$, to write the energy equation for the rotation decay when the external current is disconnected as $d(\rho v^2 h/2)/dt = -2(\sigma\mu)^{1/2}Bv^2$; this implies exponential change in the speed with time-constant $\tau_H = \rho h/[2(\sigma\mu)^{1/2}B]$.

Figure 3 shows typical curves for the potential proportional to the velocity as a function of time after current switching. When the current is switched on, the longitudinal and Hartmann layers are formed, together with the potential core. The characteristic structuring time is taken as $\Delta\tau_1$, which corresponds to the intersect on the t axis for the dashed line 4 in Fig. 3, which extrapolates the exponential part of curve 1. When the current is switched off, the flow structure alters in accordance with the change in induced-current pattern. The characteristic time here is $\Delta\tau_2$, which corresponds to the dashed line 3 in Fig. 3 intersecting the straight line $\varphi=\varphi_0$ which represents the extrapolation for the exponential part of curve 2. Figure 4 shows $\Delta\tau_1/\tau_H$ and $\Delta\tau_2/\tau_H$ as functions of Ha*. In that Ha* range, $\Delta\tau_1/\tau_H \approx \Delta\tau_2/\tau_H \approx 0.1$.

Figure 5 shows the Ha* dependence for the measured time-constants for acceleration τ_1 and decay τ_2, together with the [3, 5] data. The measured τ_i (i = 1, 2) deviate appreciably from the theoretical τ_H only for small Ha*. As h/2R increases further, so does the deviation, evidently because of effects from viscous dissipation at the central lead. This aspect requires further examination.

These results can be used to examine two-dimensional turbulent perturbation conditions in magnetic fields.

LITERATURE CITED

1. S. I. Braginskii, "Magnetohydrodynamics for weakly conducting liquids," Zh. Éksp. Teor. Fiz., 37, No. 5, 1417-1430 (1959).
2. V. B. Levin, "A free rotating layer of electrically conducting liquid in an axial magnetic field," Magn. Gidrodin., No. 1, 86-92 (1980).
3. A. A. Klyukin and V. B. Levin, "Stability in a free enclosed rotating layer of conducting liquid in an axial magnetic field," Izv. Akad. Nauk SSSR, Mekh. Zhidk. Gaza, No. 5, 116-173 (1984).

4. Kh. É. Kalis and Yu. B. Kolesnikov, "A numerical study on a single vortex in a viscous incompressible conducting liquid in an axial homogeneous magnetic field," Magn. Gidrodin., No. 2, 57-61 (1980).
5. A. A. Klyukin, "Measurements on shear flow with free boundaries in a magnetic field," Ph.D. Thesis [in Russian], Riga (1981).

0024-998X/88/2403-0385$12.50